Proceedings of ASME 201412th Biennial Conference on Engineering Systems Design and Analysis
ESDA 2014
June25-27, 2014. Copenhagen, Denmark

ESDA2014-20412

THERMODYNAMIC ANALYSIS OF A COMPRESSED AIR ENERGY STORAGE FACILITY EXPORTING COMPRESSION HEAT TO AN EXTERNAL HEAT LOAD

Hossein Safaei, Michael J. Aziz
School of Engineering and Applied Sciences,
Harvard University
Cambridge, MA, USA

ABSTRACT

Fluctuations of electric load call for flexible generation technologies such as gas turbines. Alternatively, bulk energy storage (BES) facilities can store excess off-peak electricity to generate valuable peaking electricity. Interest in electricity storage has increased in the past decade in anticipation of higher penetration levels of intermittent renewable sources such as wind. Compressed Air Energy Storage (CAES) is one of the most promising BES technologies due to the large amount of energy (hundreds of MWh) that can be economically stored. CAES uses off-peak electricity to compress air into underground reservoirs. Air is combusted and expanded at a later time to regenerate electricity. One of the downsides of CAES is the large energy losses incurred in the form of waste compression heat. Distributed CAES (D-CAES) has been proposed in order to improve the roundtrip efficiency of CAES by utilizing the compression heat for space and water heating. The compressor of D-CAES is located near a heat load (e.g. a shopping mall) and the compression heat is recovered to meet this external load. D-CAES collects fuel credits equal to the negated heating fuel, leading to a higher overall efficiency compared to conventional CAES. We perform a thermodynamic analysis of conventional CAES and D-CAES to compare their heat rate, work ratio (electric energy stored per unit of electric energy regenerated), and exergy efficiency.

1. INTRODUCTION

Bulk energy storage (BES) facilities can provide the electric grid a wide range of ancillary services such as energy arbitrage and load following. Pumped Hydroelectric Storage (PHS) plants, for example, store hundreds of MWh of excess inexpensive electricity to be discharged in peak periods. Interest in BES has been increased in the past decade as it can mitigate the variability of intermittent renewables (wind and solar) and contribute to decarbonisation efforts.

Compressed Air Energy Storage (CAES) is thought of as a promising BES technology due to the large amount of energy that can be stored at attractive costs [1]. In principle, CAES is very similar to a gas turbine (GT) with the difference being that the compression and expansion phases are decoupled in time. The compressor is powered by electricity provided by the grid in CAES and by the expander in GT. CAES stores compressed air in above or underground reservoirs. The air is later passed through combustion chambers and expanders (same as GT) to generate work. In gas turbines, roughly 50-70% of the expander output is consumed by the compressor itself [2]. Therefore, CAES can provide significantly more peaking power than a similarly sized GT because its compressor is idle during the generation phase.

Currently, two commercial CAES facilities are in operation; a few more plants are under design and construction. The first facility, located in Huntorf (Germany), stores air in a salt cavern with a volume of 310,000 m^3 in a pressure range of 46-72 bar. The Huntorf plant can produce 290 MW of electric power at full capacity for four hours. The McIntosh plant in Alabama, the second commercial CAES facility, generates 110 MW of electricity at full capacity for 26 hours. It stores air in a 560,000 m^3 salt cavern in a pressure range of 45-74 bar [1].

A major shortcoming of conventional CAES, especially if used to decarbonize the grid, is fuel combustion in the generation phase. Fuel combustion boosts the energy output of the plant, as compared to solely harnessing the mechanical energy of compressed air. Moreover, heating the compressed air is necessary to prevent the freezing of its moisture content during expansion, which would damage the turbine.

Several variations of conventional CAES have been proposed in order to reduce its heat rate. Three such designs are Adiabatic CAES (A-CAES), Isothermal CAES (I-CAES), and Distributed CAES (D-CAES). The latter is a new design recently proposed by Safaei *et al.* [3]. This paper presents a full thermodynamic analysis of a simplified CAES and D-CAES plant in order to compare various measures of their efficiency.

Section 2 provides details of the modeled systems. The thermodynamic analysis is performed in Section 3. Finally, results of a case study are discussed in Section 4.

NOMENCLATURE

ac	Approach temperature
BL	Boiler of district heating system
C_P, C_v	Specific heat at constant pressure and volume, $kJ/kg.K$
CC	Combustion chamber
ch	Charge process
CL	Inter-/ after-cooler of compressor
CM	Compressor
CN	Cavern
CR	Compression ratio
ct	Fuel credit gained by D-CAES
D	Diameter of pipeline, mm
dc	Discharge process
DH	District heating system
dn	Downstream of pipeline
em	State of a depleted cavern
et	Exhaust stream
f	Friction factor of pipeline
F	Flow rate of pipeline, m^3/day
fl	State of a full cavern
h	Specific enthalpy, kJ/kg
HC	Heat recovery unit of D-CAES
HP	High pressure equipment
HR	Heat rate, kJ/kWh
HX	Heat exchanger at the exhaust of the plant
I	Exergy loss, kJ
IP	Intermediate pressure equipment
is	Isentropic process
L	Length of pipeline, km
LHV	Low heating value, kJ/kg
LP	Low pressure equipment
m	Mass of air in cavern, kg
NG	Natural gas
P	Pressure, kPa
PP	Pipeline of D-CAES
Q	Thermal energy, kJ
R	Ideal gas constant for air, $kJ/kg.K$
RP	Recuperator
s	Specific entropy, $kJ/kg.K$
T	Temperature, K
TB	Turbine (expander)
u	Specific internal energy, kJ/kg
up	Upstream of pipeline
V	Volume of cavern, m^3
W	Work, kJ
WR	Work ratio
x	Specific exergy, kJ/kg
X	Exergy, kJ
XR	Expansion ratio
γ	Specific heat ratio of air
η	Efficiency
ρ	Exergy density of cavern, kJ/m^3
ψ	Exergy of air stream, kJ/kg

2. SYSTEMS OF STUDY

We model the conventional CAES plant illustrated in Fig. 1 and the D-CAES plant illustrated in Fig. 2.

2.1 CONVENTIONAL CAES DESIGN

In the conventional CAES system (Fig. 1), air is compressed in a multi-stage compressor and stored in an underground reservoir. Each compression stage is followed by a cooler to reduce the compression work of the next stage and to reduce the volume of storage required. Conventional CAES plants dump this heat to the ambient. We model a constant volume cavern (similar to the Huntorf and McIntosh plants); therefore, the pressure of the cavern varies between a lower and upper bound during the charge and discharge process. In order to maintain its mechanical integrity and to ensure high enough flow rates of the air being withdrawn, the cavern is never fully depleted. The minimum air mass remaining at the end of the discharge phase, when all the working air has been withdrawn to generate electricity, is called the “cushion air”.

Air is withdrawn from the cavern and preheated in a recuperator during the discharge period. It is then combusted with fuel (natural gas in our case) prior to generating mechanical energy in the expanders. We model a two-stage expansion train. Through a recuperator, the exhaust of the low pressure turbine preheats air entering the high pressure combustion chamber. The Huntorf and McIntosh plants both use this CAES design except that the Huntorf plant is not equipped with a recuperator.

Adiabatic CAES (A-CAES) and Isothermal CAES (I-CAES) are among newer designs that aim to reduce the fuel consumption of CAES. The main characteristic of A-CAES is complete elimination of the combustors through storage and utilization of high exergy compression heat. Theoretically, if high temperature heat is generated through compressing air to high pressures and this high exergy heat is stored in a thermal energy storage (TES) facility, the stored heat could eliminate the need for burning fuel during the discharge period. More about A-CAES may be found in [4-6]. Development of A-CAES is, nevertheless, technologically and economically challenged with the need for high pressure and high

temperature TES and compressors and high pressure expanders at large scale [7]. General Electric and five other industry partners are developing an A-CAES pilot project called "ADELE" which may start operation by 2016 in Germany [8].

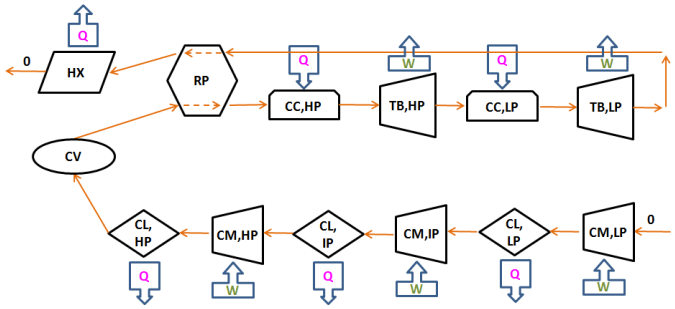

Fig. 1 Schematic of the modeled CAES system. "Q" and "W" represent heat and work interactions between the system and the surroundings. "0" indicates ambient condition.

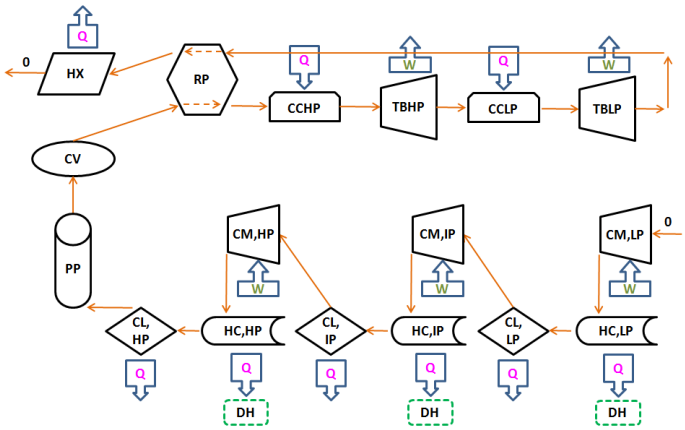

Fig. 2 Schematic of the modeled D-CAES system. A portion of the compression heat is recovered and exported to a district heating (DH) system to meet a heat load and gain fuel credits for the D-CAES plant. Not all the compression heat is suitable for district heating. The heat recovered by the coolers is dumped to the ambient due to its low temperature.

I-CAES, in contrast, relies on near-isothermal compression and expansion of air. Isothermal compression requires the least compression energy and isothermal expansion requires no fuel. Such a system needs to remain in close thermal equilibrium with the surroundings. Approaching this equilibrium has, to date, proven impractical for large scale I-CAES plants, as both processes must happen very slowly or an unrealistically large heat transfer area must exist[1].

[1]Another possibility is having a very large number of compression stages and after-coolers to achieve nearly isothermal compression. Obviously, there exists a trade-off between number of compression stages (capital cost) and compression work (operating cost). A similar argument can be made for multi-stage expanders.

2.2 DISTRIBUTED CAES (D-CAES) DESIGN

As shown in Fig. 2, the D-CAES concept utilizes the low exergy compression heat of a conventional CAES plant for space and water heating – an application that does not require high exergy heat, although fuel is often burned for it. The main idea here is to export the waste heat of compression to satisfy an external municipal heat load[2] and to gain credit for the negated consumption of heating fuel. Note that D-CAES still uses fuel (at levels similar to conventional CAES); nevertheless, it has a lower net heat rate once fuel credits are taken into account. Underground storage facilities are geographically constrained due to geological requirements for air storage such as permeability and porosity of the reservoir. Therefore, D-CAES requires a suitable geological formation (to host the cavern) in proximity to a concentrated heat load (to consume the otherwise wasted heat of compression). Hence, D-CAES is anticipated to be economically viable only in niche markets where both of these requirements are met [9].

Fig. 2 illustrates the D-CAES system analyzed in this paper. The compressor is located within the city to provide its compression heat to a district heating (DH) system in order to meet a space and water heating load. The expander is co-located with the cavern, similar to conventional CAES. A pipeline is therefore required to transport air from the compression site to the storage site. Note that air should be compressed to higher pressures in order to compensate losses along the pipeline. Tradeoffs between pipeline capital cost, additional compression work, and fuel credits ultimately determine economic competitiveness of D-CAES with CAES.

The thermodynamics of CAES has been extensively studied [10-13], but that of D-CAES has not been evaluated in detail. This paper fills this gap by performing a full exergy analysis of CAES and D-CAES to quantify several thermodynamic figures of merit as a function of selected design parameters (pipeline length, cavern pressure, and throttling the withdraw air to a fixed pressure).

One should note that round-trip storage efficiency is widely used as the standard parameter comparing the efficiency of various storage technologies. It is defined as the electrical energy generated per unit of electrical energy taken in. Nevertheless, CAES and D-CAES use both electrical energy (to run the compressor and charge the cavern) and heating energy (natural gas for air combustion and expansion). Consequently, we use three key performance parameters to fully describe the thermodynamic performance of CAES and D-CAES: heat rate, work ratio, and exergy roundtrip efficiency. The heat rate equals the amount of natural gas combustion heat (LHV) used by the plant per unit of electrical energy generated. This parameter is specifically important when emissions are constrained (the main motivation for the A-CAES and I-CAES designs, with heat rates of zero). The work ratio equals the electrical energy consumed by the compressor per unit of electrical energy generated by the expander. The work ratio is

[2] The waste heat of compression may also provide cooling energy through absorption chilling technologies.

especially important when off-peak electricity is constrained or expensive. Finally, the exergy efficiency combines heat rate and work ratio into one parameter characterizing exergy losses incurred over the storage process. As shown in (34), (43), and (46), we define the exergy efficiency as the ratio of the useful exergy delivered by the plant (expansion work) to the net exergy provided to the plant. The net exergy consumed by the plant is the summation of the compression work and the exergy of fuel burned in the combustors (minus the fuel exergy credit from export of waste heat in the D-CAES system).

3. THERMODYNAMIC ANALYSIS

Following are the general assumptions/ simplifications used in thermodynamic analysis of CAES and D-CAES.

One complete charge/discharge cycle is analyzed, with no partial load operation. Air is modeled as an ideal gas with temperature-independent thermodynamic properties. The ambient (subscript 0) is at $P_0 = 101$ kPa, $T_0 = 298$ K. This condition is also the reference state for enthalpy and entropy calculations.

The cavern has a fixed volume and variable pressure. The minimum pressure of the cavern, P_{em}, corresponds to a fully depleted cavern (at the beginning of the charge process and the end of the discharge process). Maximum pressure, P_{fl}, corresponds to a fully charged cavern (end of the charge process and beginning of the discharge process). The cavern and pipeline are assumed adiabatic and isothermal, respectively.

The exhaust temperature of the plant (T_{et}) is fixed throughout the operation. Following Osterle [10], an imaginary heat exchanger (HX) is located after the exhaust of the storage plant (inside the control volume) to account for the loss of the exergy of the exhaust stream to the ambient. This device cools down the exhaust stream from T_{et} to the ambient temperature. The analyzed control volume includes the storage plant and this heat exchanger (i.e. the entire system shown in Fig. 1 and Fig. 2, except the DH system). Equations (1) to (5) list the ideal gas formulae applied to air in this study.

$$m_{CN} = \frac{P_{CN} \times \mathrm{V}}{R \times T_{CN}} \quad \text{Mass of air in cavern} \tag{1}$$

$$h = C_p \times (T - T_0) \quad \text{Enthalpy of air} \tag{2}$$

$$s = C_p \ln\left(\frac{T}{T_0}\right) - R \ln\left(\frac{P}{P_0}\right) \quad \text{Entropy of air} \tag{3}$$

$$u = C_v \times T - C_p \times T_0 \quad \text{Internal energy of air} \tag{4}$$

$$\psi = (\mathrm{h} - \mathrm{h}_0) - \mathrm{T}_0(\mathrm{s} - \mathrm{s}_0) \quad \text{Stream exergy of air} \tag{5}$$

Note that that all the heats (Q) are reckoned positive if they enter the system (e.g. Q_{CC}) and negative if they leave the system (e.g. Q_{HC}). The work (W) done by the system on the surroundings has a positive sign (e.g. W_{TB}) whereas the work done on the system has a negative sign (e.g. W_{CM}).

3.1 THERMODYNAMIC ANALYSIS OF CAES

We use the following specific assumptions in modeling CAES.

The compressor has three stages; low (LP), intermediate (IP), and high pressure (HP). All three stages have variable but equal compression ratios and fixed isentropic efficiencies. The compression ratio, CR_{CM} varies to match the instantaneous pressure of the cavern (P_{CV}). Therefore, $CR_{CM,HP} = CR_{CM,IP} = CR_{CM,LP} = \sqrt[3]{\frac{P_{CN}}{P_0}} = \sqrt[3]{CR_{CM}}$.

Coolers are assumed to have a fixed approach temperature, defined as the difference between temperature of the hot stream leaving the cooler and the cooling fluid entering the cooler: $\mathrm{T_{ac}} = \mathrm{T^{CL}_{out,hot}} - \mathrm{T^{CL}_{in,cold}}$ (see Fig. 3). Note this assumption implies the inlet temperature of the cavern and the output of all three coolers are fixed through the charging process and equal to $\mathrm{T_{ac}} + \mathrm{T^{CL}_{in,cold}} = \mathrm{T_{ac}} + T_0 = T_{out,hot}$.

The discharge temperature of both combustion chambers is fixed (through controlling fuel combustion). High and low pressure expanders have equal but variable expansion ratios to match the instantaneous cavern pressure:

$$XR_{TB,HP} = XR_{TB,LP} = \sqrt{\frac{P_0}{P_{CN}}} = \sqrt{XR_{TB}}.$$

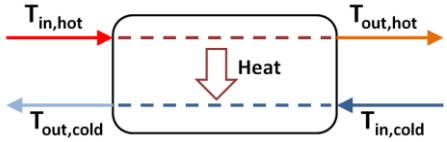

Fig. 3 Schematic of compressor's cooler. The hot stream is the exhaust of each compression stage and the cold stream represents an external cooling fluid taking the heat out of the system. The approach temperature is defined as: $\mathbf{T_{ac} = T_{out,hot} - T_{in,cold}}$

3.1.1 CHARGE PHASE OF CAES

At the beginning of each charging process, the initial temperature and pressure of the cavern are known from the previous cycle. Therefore, the mass of the cushion air is calculated by applying the ideal gas equation of state. The relationship between the change in the mass of air present in the cavern and its instantaneous pressure is found by applying the First Law of Thermodynamics to the control volume of the cavern:

$$dQ - dW = dU_{CV} - dm_{in} \times h_{in}$$

Because the cavern is adiabatic and at constant volume, $dQ = dW = 0$. Using (1), (2), and (4), the above equation results in (6).

$$dm_{ch} = \frac{dP_{ch} \times \mathrm{V}}{R \times \gamma \times T_{in}^{CV}} \tag{6}$$

Because the inlet temperature of the cavern, T_{in}^{CN} is fixed, (6) is integrated to find the total mass of air injected during the charge process (working air), as shown in (7). The temperature of the fully charged cavern is determined by

applying the First Law to the cavern over the charging process or, alternatively, by applying (1), as shown in (8).

$$m_{ch} = \frac{\left(P_{fl} - P_{em}\right) \times \mathrm{V}}{R \times \gamma \times T_{in}^{CN}} \tag{7}$$

$$Q - W = m_{fl} \times u_{CN,fl} - m_{em} \times u_{CN,em} - m_{ch} \times h_{in}^{CN} \rightarrow$$

$$T_{CN,fl} = \frac{T_{CN,em} \times P_{fl}}{P_{em} + (P_{fl} - P_{em}) \times \frac{T_{CN,em}}{\gamma \times T_{in}^{CN}}} \tag{8}$$

The compression work required to fully charge the cavern is quantified by applying the First Law to each compression stage and summing them up (equation (10)). Equation (9) shows the energy consumption of the *LP* compressor. Similar formulae are applicable to the *IP* and *HP* compressors. Note that the inlet temperature of each stage is fixed and known.

$$dW_{CM,LP} = dm_{ch} \times C_p\left(T_{in}^{CM,LP} - T_{out}^{CM,LP}\right) \tag{9}$$

$$T_{out}^{CM,LP} = T_{in}^{CM,LP} - \frac{T_{in}^{CM,LP} - T_{out,is}^{CM,LP}}{\eta_{is}^{CM,LP}}$$

$$T_{out,is}^{CM,LP} = T_{in}^{CM,LP} \times CR_{CM,LP}^{(\gamma-1)/\gamma}$$

$$W_{CM} = \int_{\mathrm{P_{em}}}^{\mathrm{P_{fl}}} \left(dW_{CM,LP} + dW_{CM,IP} + dW_{CM,HP}\right) \tag{10}$$

The heat dissipated by intercoolers and aftercooler is quantified by applying the First Law to each cooler. As a case in point, (11) represents an increment of heat dissipated by the *LP* intercooler. Eq. (12) represents the total compression heat that is lost to the ambient in the CAES system.

$$dQ_{CL,LP} = dm_{ch} \times C_p\left(T_{in}^{CL,LP} - T_{out}^{CL,LP}\right) \tag{11}$$

$$Q_{CL} = \int_{\mathrm{P_{em}}}^{\mathrm{P_{fl}}} \left(dQ_{CL,LP} + dQ_{CL,IP} + dQ_{CL,HP}\right) \tag{12}$$

Since the initial and final states of the cavern and the compression energy are now known, the total exergy loss of the charging phase is quantified by (16).

$$\Delta U_{ch}^{CN} = m_{fl} \times u_{CN,fl} - m_{em} \times u_{CN,em} \tag{13}$$

$$\Delta S_{ch}^{CN} = m_{fl} \times s_{CN,fl} - m_{em} \times s_{CN,em} \tag{14}$$

$$\Delta X_{ch}^{CN} = \Delta U_{ch}^{CN} - T_0 \times \Delta S_{ch}^{CN} \tag{15}$$

$$I_{ch} = -\Delta X_{ch}^{CN} - W_{CM} + m_{ch} \times \psi_0 \tag{16}$$

Note that $\psi_0 = 0$ according to (5).

3.1.2 DISCHARGE PHASE OF CAES

Similar to the charging phase, the First Law is applied to the cavern in order to determine the relationship between its instantaneous pressure, instantaneous temperature and change in the mass of the stored air.

$$dm_{dc} = \frac{dP_{CN} \times \mathrm{V}}{R \times \gamma \times T_{CN}} \tag{17}$$

Using (17) and (1), we find the mass of stored air in the fully discharged cavern (equation (18)) and the mass of air withdrawn (equation (19)). The temperature of the fully discharged cavern is determined by applying the isentropic process relationship for an ideal gas with temperature-independent specific heats, equation (20). We set the initial temperature of the fully discharged cavern to T_0. This temperature eventually reaches asymptotic limits after many cycles, regardless of the initial temperature of the cavern in the first cycle. Simulation is run until this asymptotic limit is reached and all the results reported here correspond to this asymptotic limit.

$$\frac{dm_{dc}}{m_{dc}} = \frac{dP_{CN}}{\gamma \times P_{CN}} \rightarrow$$

$$m_{em} = m_{fl} \times \left(\frac{P_{em}}{P_{fl}}\right)^{\frac{1}{\gamma}} \tag{18}$$

$$m_{dc} = m_{fl} - m_{em} = m_{fl} \times \left(1 - \left(\frac{P_{em}}{P_{fl}}\right)^{\frac{1}{\gamma}}\right)$$

$$m_{dc} = \left(\frac{\mathrm{V} \times P_{em}}{R \times T_{em}} + \frac{\mathrm{V}\left(P_{fl} - P_{em}\right)}{R \times \gamma \times T_{in}^{CN}}\right) \times \left(1 - \left(\frac{P_{em}}{P_{fl}}\right)^{\frac{1}{\gamma}}\right) \tag{19}$$

$$T_{em} = T_{fl} \times \left(\frac{P_{em}}{P_{fl}}\right)^{(\gamma-1)/\gamma} \tag{20}$$

The fundamental assumption in our analysis of the expansion stage is that it may be modeled as a control mass of air, stored in the cavern, undergoing a reversible and adiabatic (isentropic) expansion as its pressure drops from P_{fl} to P_{em}. Therefore, (21) relates the instantaneous temperature of the cavern (T_{CN}) to its instantaneous pressure (P_{CN}).

$$T_{CN} = T_{fl} \times \left(\frac{P_{CN}}{P_{fl}}\right)^{(\gamma-1)/\gamma} \tag{21}$$

As discussed earlier, the inlet temperatures of both turbines ($T_{in}^{TB,LP}$ and $T_{in}^{TB,HP}$) are fixed. However, the exhaust temperature depends on the instantaneous expansion ratio, which is a function of the cavern's instantaneous pressure. We apply the First Law to find the work done by the high pressure and low pressure turbines, as shown in (22) and (23).

$$T_{out}^{\mathrm{TB},HP} = T_{in}^{TB,HP} + \eta_{is}^{TB,HP}\left(T_{out,is}^{TB,HP} - T_{in}^{TB,HP}\right) \tag{22}$$

$$T_{out,is}^{TB,HP} = T_{in}^{TB,HP} \times XR_{TB,HP}^{(\gamma-1)/\gamma}$$

$$dW_{TB,HP} = C_p\left(T_{in}^{TB,HP} - T_{out}^{\mathrm{TB},HP}\right) \times dm_{dc}$$

$$W_{TB} = \int_{\mathrm{P_{fl}}}^{\mathrm{P_{em}}} \left(dW_{TB,HP} + dW_{TB,LP}\right) \tag{23}$$

where $XR_{TB,HP} = XR_{TB,LP} = \sqrt{\frac{P_0}{P_{CN}}} = \sqrt{XR_{TB}}$.

Now that the instantaneous discharge temperature of the high pressure expander is determined as a function of the instantaneous cavern pressure, the heat added in the low pressure combustor is determined by applying the First Law, as shown in (24). Note that $T_{in}^{CC,LP} = T_{out}^{TB,HP}$ and $T_{out}^{CC,LP} = T_{in}^{TB,LP}$.

$$dQ_{CC,LP} = C_p(T_{out}^{CC,LP} - T_{in}^{CC,LP}) \times dm_{dc}$$

$$Q_{CC,LP} = \int_{P_{fl}}^{P_{em}} dQ_{CC,LP} \quad (24)$$

One can apply the First Law to the recuperator to determine the instantaneous temperature of the air entering the high pressure combustor as a function of the cavern's pressure (equation (25)). The heat added in the high pressure combustor can therefore be calculated by (26). Note that $T_{out}^{CC,HP} = T_{in}^{TB,HP}$.

$$T_{in}^{CC,HP} = T_{CN} + T_{out}^{TB,LP} - T_{et} \quad (25)$$

$$dQ_{CC,HP} = C_p(T_{out}^{CC,HP} - T_{in}^{CC,HP}) \times dm_{dc}$$

$$Q_{CC,HP} = \int_{P_{fl}}^{P_{em}} dQ_{CC,HP} \quad (26)$$

where T_{et} is the exit temperature of the exhaust of the recuperator.

Heat recovered in the recuperator and heat dissipated in the exhaust heat exchanger are quantified by (27) and (28).

$$Q_{RP} = \int_{P_{fl}}^{P_{em}} C_p(T_{et} - T_{out}^{TB,LP}) \times dm_{dc} \quad (27)$$

$$Q_{HX} = \int_{P_{fl}}^{P_{em}} C_p(T_0 - T_{et}) \times dm_{dc} \quad (28)$$

Now that the heat added in each combustor is determined (equations (24) and (26)), the exergy supplied to the storage plant by fuel is expressed by (29).

$$X_{NG}^{dc} = (Q_{LP,CC} + Q_{HP,CC}) \times x_{NG}/LHV_{NG} \quad (29)$$

Finally, the exergy loss in the discharge process is calculated by (33).

$$\Delta U_{dc}^{CN} = m_{em} \times u_{CN,em} - m_{fl} \times u_{CN,fl} \quad (30)$$

$$\Delta S_{dc}^{CN} = m_{em} \times s_{CN,em} - m_{fl} \times s_{CN,fl} \quad (31)$$

$$\Delta X_{dc}^{CN} = \Delta U_{dc}^{CN} - T_0 \times \Delta S_{dc}^{CN} \quad (32)$$

$$I_{dc} = -\Delta X_{dc}^{CN} - W_{TB} + X_{NG}^{dc} - m_{dc} \times \psi_0 \quad (33)$$

3.1.3 FULL CYCLE OF CAES

Once the energy and exergy inputs and outputs are determined, the roundtrip efficiency, work ratio and heat rate are calculated by applying (34) to (36).

$$\eta_{X,CAES} = \frac{W_{TB}}{-W_{CM} + X_{NG}^{dc}} \quad (34)$$

$$WR_{CAES} = \frac{-W_{CM}}{W_{TB}} \quad (35)$$

$$HR_{CAES} = \frac{Q_{CC}}{W_{TB}} \times 3{,}600 \quad (36)$$

3.2 THERMODYNAMIC ANALYSIS OF D-CAES

As shown in Fig. 2, the discharge process of the D-CAES plant is identical to that of the CAES system (Section 3.1.2). The difference with CAES is that a portion of the compression heat is recovered, via three heat recovery units (HC), and used in a district heating (DH) system. This otherwise wasted heat of compression earns fuel credits for the D-CAES plant equal to the saved fuel. We make the following simplifications in modeling D-CAES.

Each of the three compressors is followed by a Heat Recovery Unit (HC) and then a Cooler (CL), as illustrated in Fig. 4 for the intermediate compressor. Heat recovery units cool the compressor exhaust to a fixed temperature, T_{out}^{HC}. This absorbed heat is utilized by the DH plant. The compressed air stream is then passed through inter- and after-coolers to further cool it down. As in the CAES model, the exhaust temperature of the coolers is equal to ambient temperature plus the approach temperature.

A pipeline transports compressed air to the storage site located at some distance, L_{PP}. The compressor pressurizes air enough to compensate losses along the pipeline so that the cavern pressure can vary between P_{em} and P_{fl}, similar to CAES. The pipeline is assumed to be isothermal: $T_{up}^{PP} = T_{dn}^{PP} = T_{out}^{CL,HP}$.

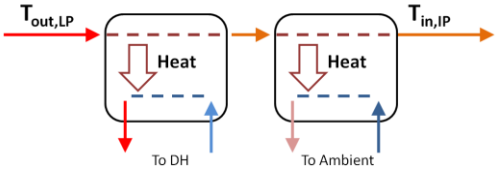

Fig. 4 Configuration of the heat recovery unit and intercoolers following each compression stage

3.2.1 CHARGE PHASE OF D-CAES

Similar to Section 3.1.1 for CAES, (7) expresses the mass of working air and (8) determines the temperature of the fully charged cavern. In D-CAES, however, the compressor needs to compensate for pressure drops along the pipeline to reach the same cavern pressure as CAES. (37) relates the pipeline pressure drop to the important pipeline characteristics [14]. Our approach to calculate the total compression work is based on using (37) to determine the upstream pressure of the pipeline, P_{PP}^{up} (equal to $P_{out}^{CM,HP}$), at each cavern pressure P_{CN}. The instantaneous compression ratio is given by $CR_{CM} = P_{PP}^{up}/P_0$. (10) is then applied to determine the total compression work.

For a set compressor size ($\dot{W}_{CM}$), a series of calculations is performed to find the compressor flow rate and discharge pressure that lead to the desired downstream pressure, which is equal to the cavern pressure and varies between P_{em} and P_{fl}. As shown in Section 4, a linear function approximates this relationship relatively well.

$$P_{up}^2 - P_{dn}^2 = 9.4 \times 10^4 \times \frac{T_{PP} \times L \times f \times F^2}{D^5} \quad (37)$$

The compression stages of D-CAES are followed by two heat exchangers to cool the air prior to entering the next stage (or pipeline), as shown in Fig. 4. Similar to CAES, heat transferred in the coolers is quantified by the First Law. (38) illustrates this for the low pressure cooler. (39) therefore represents total heat released to the ambient by the low, intermediate, and high pressure coolers.

$$dQ_{CL,LP} = dm_{ch} \times C_p \times (T_{out}^{HC,LP} - T_{out}^{CL,LP}) \quad (38)$$

$$Q_{CL} = \int_{P_{em}}^{P_{fl}} \left(dQ_{CL,LP} + dQ_{CL,IP} + dQ_{CL,HP}\right) \quad (39)$$

Similarly, heat absorbed in heat recovery units is quantified by applying the First Law, as shown in (40) for the low pressure heat recovery unit. Finally, (41) quantifies the total recovered heat that is offered to the district heating system. The exergy credit due to heat recovery is expressed by (42). η_{HC} is the percentage of the recovered heat that is utilized by the district heating system. η_{BL} is the efficiency of the boiler of the district heating system which, due to importing waste heat from D-CAES, now uses less fuel.

$$dQ_{HC,LP} = dm_{ch} \times C_p (T_{out}^{HC,LP} - T_{out}^{CM,LP}) \quad (40)$$

$$Q_{HC} = \int_{P_{em}}^{P_{fl}} (dQ_{LP} + dQ_{IP} + dQ_{HP}) \quad (41)$$

$$X_{NG}^{ct} = \frac{Q_{HC}}{LHV_{NG}} \times \frac{\eta_{HC}}{\eta_{BL}} \times x_{NG} \quad (42)$$

(13) to (15) are used to evaluate the change in internal energy, entropy, and exergy of the D-CAES cavern. (16) is used to evaluate the exergy lost in the charging process.

3.2.2 DISCHARGE PHASE OF D-CAES

The discharge process of D-CAES is identical to that modeled for the CAES configuration in Section 3.1.2.

3.2.3 FULL CYCLE OF D-CAES

One can determine the exergy efficiency, work ratio and heat rate of the D-CAES plant by applying (43), (44), and (45), respectively. However, when fuel credits from exporting recovered heat are taken into account, the net exergy efficiency and heat rate are determined by (46) and (47), respectively. Note that heat recovery lowers the net fuel consumption of the D-CAES plant (reduced heat rate), while the pipeline losses increase the compression work required to charge the cavern (elevated work ratio). Therefore, net change in the exergy efficiency of D-CAES depends on the trade-off between these two opposing factors.

$$\eta_{X,D-CAES}^{Raw} = \frac{W_{TB}}{-W_{CM} + X_{NG}^{dc}} \quad (43)$$

$$ER_{D-CAES} = \frac{-W_{CM}}{W_{TB}} \quad (44)$$

$$HR_{CAES} = \frac{Q_{CC}}{W_{TB}} \times 3{,}600 \quad (45)$$

$$\eta_{X,D-CAES}^{Net} = \frac{W_{TB}}{-W_{CM} + X_{NG}^{dc} - X_{NG}^{cr}} \quad (46)$$

$$HR_{D-CAES}^{Net} = \frac{Q_{CC} + Q_{HC} \times \frac{\eta_{HC}}{\eta_{BL}}}{W_{TB}} \times 3{,}600 \quad (47)$$

4. NUMERICAL EXAMPLE

4.1 BASE CASE SIMULATION

This section provides a case study comparing thermodynamic performance of CAES and D-CAES. Table 1 illustrates the inputs used in this example. (48) shows the relationship between the cavern pressure and the upstream pressure of the pipeline (equal to the discharge pressure of the compressor), using the values listed in Table 1 and the methodology explained in Section 3.2.1. This determines the instantaneous compression ratio used in (10) to calculate the compression energy of D-CAES.

$$P_{PP}^{up} = 0.764 \times P_{CV} + 2{,}225 \quad (48)$$

$$R^2 = 0.999$$

Table 1 Input parameters for the numerical example

Parameter	Value	Parameter	Value
$\boldsymbol{\gamma}$	1.4	V	0.56 Mm^3
$\boldsymbol{C_p}$	1.006 $kJ/(kg.K)$	η_{is}^{TB}	85%
$\boldsymbol{P_{fl}}$	7 MPa	η_{HC}	100%
$\boldsymbol{P_{em}}$	5 MPa	η_{BL}	80%
$\boldsymbol{\eta_{is}^{CM}}$	85%	T_{out}^{HC}	$100°C$
$\boldsymbol{T_{ac}}$	$30°C$	T_{PP}	$55°C$
$\boldsymbol{T_{in}^{TB,HP}}$	$530°C$	$\dot{W}_{CM}$	105 MW
$\boldsymbol{T_{in}^{TB,LP}}$	$850°C$	D_{PP}	0.75 m
$\boldsymbol{T_{et}}$	$130°C$	L_{PP}	50 km
$\boldsymbol{T_{in,cold}^{CL}}$	$25°C$	f_{PP}	0.01

Using these values, key thermodynamic outputs of the simulation are shown in Table 2. As expected, the energy requirement of D-CAES to fully charge the cavern is higher. It is of note that not all the compression heat is useful to the district heating system due to its too low temperature. Here, we have assumed that the heat exchanger to the district heating system is characterized by an approach temperature of $30°C$, implying the hot compressed air is cooled down to $T_{out}^{HC} = 100°C$, corresponding to a cold stream of $70°C$. The fuel exergy credit (4,155 GJ) is higher than the recovered heat (3,321 GJ) due to an assumed 80% boiler efficiency of the district heating facility. The higher compression requirements of D-CAES compared to CAES result in 11% higher exergy losses over the charging period. Nevertheless, the exergy credit from heat recovery (X_{NG}^{ct}=4,155 GJ) is 21 times as large as the additional exergy losses (I_{ch}) endured to charge the cavern of D-CAES (1,775 GJ) compared to CAES (1,580 GJ). The

discharge phases of CAES and D-CAES have the same characteristics.

D-CAES has a higher work ratio (0.766 vs. 0.738) due to pressure losses in the pipeline. The simulated D-CAES plant consumes approximately 3 more units of electrical energy compared to CAES to generate 100 units of electrical energy. Both plants have moderate values of the raw exergy efficiency (54.3% and 53.5%, respectively), which are in the lower spectrum of bulk energy storage technologies. Pumped hydro storage, for example, has a round-trip storage efficiency of about 80% [15].

Table 2 Simulation results of thermodynamic analysis of CAES and D-CAES systems in the base case

Variable	CAES	D-CAES	Unit
W_{CM}	-4,557	-4,732	GJ
Q_{HC}	0	-3,321	GJ
X_{NG}^{ct}	0	4,155	GJ
I_{ch}	1,580	1,755	GJ
W_{TB}	6,179	6,179	GJ
Q_{CC}	6,820	6,820	GJ
X_{NG}^{dc}	6,826	6,826	GJ
I_{dcg}	3,624	3,624	GJ
WR	0.738	0.766	NA
η_X^{Raw}	54.3	53.5	%
HR^{Raw}	3,974	3,974	kJ/kWh
η_X^{Net}	54.3	83.5	%
HR^{Net}	3,974	1,555	kJ/kWh

Nevertheless, D-CAES looks significantly stronger once the fuel credits are taken into account. It reaches a net efficiency of 83.5% and a net heat rate of 1,555 kJ/kWh. This occurs because approximately 70% of the energy consumed by the compressor (W_{CM}=4,732 GJ) is recovered and is utilized by the district heating system (Q_{HC}=3,321 GJ). These results provide an optimistic view of D-CAES performance. We have assumed that all the recovered heat in the heat recovery units is consumed by the district heating system and earns fuel credits for D-CAES (i.e. $\eta_{HC} = 100\%$). In case of excess recovered heat beyond the district heating's instantaneous demand, it needs to be dumped to the ambient or stored in a thermal energy storage system for later use, both of which would degrade the efficiency of D-CAES.

4.2 SENSITIVITY TO PIPELINE LENGTH

A key parameter in economic viability of D-CAES is the distance between the compressor and the cavern, as pipeline projects are capital intensive [3]. This distance impacts the thermodynamic performance of D-CAES as well, due to the dependence of the pressure losses on pipeline length. The sensitivity of the results to pipeline length when all other parameters are kept the same is shown in Table 3. A longer pipeline requires more compression energy (higher work ratio); nevertheless, it provides more heat recovery opportunities (higher Q_{CH}). The work ratio varies from 0.753 to 0.787 when the pipeline length varies from 25 to 100 km, as compared to a value of 0.738 for CAES. The net effect of higher W_{CM} and Q_{HC} is marginal on the exergy efficiency as the D-CAES pipeline length increases.

Table 3 Sensitivity of performance metrics to pipeline length

Parameter	CAES	25 km	50 km	75 km	100 km
W_{CM}(GJ)	-4,557	-4,652	-4,732	-4,800	-4,861
X_{NG}^{ct}(GJ)	0	4,055	4,155	4,241	4,317
WR	0.738	0.753	0.766	0.777	0.787
η_X^{Raw}(%)	54.3	53.8	53.5	53.1	52.9
η_X^{Net}(%)	54.3	83.2	83.5	83.7	83.8
HR^{Net}(kJ/kWh)	3,974	1,613	1,555	1,505	1,461

4.3 SENSITIVITY TO STORAGE PRESSURE

Another key parameter is the pressure range of the cavern. We varied the max cavern pressure from 7 to 11 MPa while the minimum pressure was kept at 5 MPa (see Table 4). With increasing max cavern pressure from the base case value of P_{fl}=7 MPa, the work ratio of both plants rises as higher compression losses are incurred to charge the cavern. Nevertheless, the work ratio of D-CAES is less sensitive to increases in the maximum cavern pressure compared to that of CAES. This is because pipeline losses (P_{up}-P_{dn} in (37)) are lower at higher pipeline pressures and also because of the decreased flow rates in the pipeline (the size of the compressor is kept constant so the flow rate is lower at higher pipeline pressures). Higher compression losses incurred at elevated cavern pressures lower the exergy efficiency of CAES compared to the base case (P_{fl}=7 MPa and η_X^{Net}=54.3%). Nevertheless, the net exergy efficiency of D-CAES improves at elevated cavern pressures, compared to the base case (P_{fl}=7 MPa and η_X^{Net}=83.6%), because additional heat recovery opportunities and lower pipeline losses outweigh increased compression losses.

The net effect of increasing the maximum pressure of the cavern is to reduce the heat rate of the D-CAES plant compared to the base case (P_{fl}=7). The heat rate of CAES is not sensitive to this change. Despite exergy efficiency penalties, higher storage pressures may become an appealing option as they increase the exergy density of the cavern. Raising the maximum cavern pressure from 7 to 11 MPa approximately triples the volumetric exergy density, defined as the ratio of total expansion energy to cavern volume.

Table 4 Sensitivity of results to cavern upper pressure

	7 MPa		9 MPa		11 MPa	
	CAES	DCAES	CAES	DCAES	CAES	DCAES
WR	0.738	0.760	0.751	0.770	0.763	0.775
η_X^{Raw}	54.3	53.7	54.0	53.4	53.7	53.3
η_X^{Net}	54.3	83.6	54.0	84.2	53.7	84.8
HR^{Net}	3,974	1,570	3,965	1,503	3,958	1,453
ρ	11,033		22,611		34,583	

4.4 EXPANDER WITH CONSTANT INLET PRESSURE

We have assumed in the base case that the inlet pressure of expanders and, consequently, their expansion ratios, vary as air is withdrawn from the cavern. Another possibility is, however, to throttle withdrawn air in order to maintain a fixed inlet pressure for the expanders. Despite the exergy losses of throttling and a lower exergy density of the cavern in this situation, both the Huntorf and the McIntosh plants utilize such a design due to both higher efficiencies of turbines with fixed expansion ratios [1] and in order to keep the power output of the CAES plant constant [16]. The Huntorf plant throttles withdrawn air to 46 bar (with the cavern operating between 46 and 72 bar) whereas the McIntosh plant throttles withdrawn air to 45 bar (with the cavern pressure operating between 45 and 74 bar).

It is reasonable to assume that future CAES plants will avoid throttling losses if CAES technology is implemented on a large scale (due to the need for increasing the cavern exergy density and the storage efficiency) and to assume that this will be facilitated by technological improvements in expander design. In order to assess the effect of throttling on the thermodynamics of CAES and D-CAES, we repeated the simulation with constant expansion ratios. Air withdrawn from the cavern is throttled to P_{em} prior to entering the recuperator. Because this process involves no work or heat transfer, it is isenthalpic. Since air is modeled as an ideal gas, an isenthalpic process does not change its temperature. Therefore, all the previous formulae are still applicable with the difference that a fixed expansion ratio (equation (49)) is now used in (22) and (23) in order to determine the work generated by the expanders.

$$XR_{TB,HP} = XR_{TB,LP} = \sqrt{\frac{P_0}{P_{em}}} = \sqrt{XR_{TB}} \tag{49}$$

Table 5 reports key thermodynamic parameters of CAES and D-CAES with and without throttling, using values of $P_{em} = 5\ MPa$, $P_{fl} = 7\ MPa$, and $L = 50\ km$. Throttling reduces the expansion energy of both CAES and D-CAES by 3% (5,982 GJ compared to 6,179 GJ in the base case scenario). The exergy density of the cavern is also decreased by 3% (10,681 GJ/m^3 compared to 11,033 GJ/m^3). Nevertheless, throttling lowers the fuel consumption of both plants by approximately 3% as well (6,623 GJ from the base value of 6,820 GJ) because the expansion ratio of the expanders is now reduced. Throttling increases the work ratio of CAES to 0.762 compared to the base case value of 0.738. A similar effect is observed for D-CAES: throttling increases the work ratio from 0.766 to 0.791. The net effect of a lower expansion energy and fuel consumption is insignificant on the heat rate of CAES, whereas it improves the net heat rate of D-CAES by approximately 4% (1,487 compared to 1,555 kJ/kWh). The CAES and D-CAES plants modeled here have exergy efficiencies of 53.5% and 83.0%, respectively, when withdrawn air is throttled to keep expansion ratios of the expanders constant. These are slightly lower than the respective corresponding values of 54.3% and 83.5% without throttling.

Table 5 Effect of throttling on performance of CAES and D-CAES. "Var. P" represents the case with variable expansion ratios while "Throttle" indicates constant expansion ratios

Parameter	CAES		D-CAES	
	Var. P	Throttle	Var. P	Throttle
W_{CM}(GJ)	-4,557	-4,557	-4,732	-4,732
X_{NG}^{ct}(GJ)	0	0	4,155	4,155
W_{TB} (GJ)	6,179	5,982	6,179	5,982
Q_{CC} (GJ)	6,820	6,623	6,820	6,623
X_{NG}^{Net}(GJ)	6,826	6,628	2,671	2,473
WR	0.738	0.762	0.766	0.791
η_X^{Net}(%)	54.3	53.5	83.5	83.0
HR^{Net}(kJ/kWh)	3,974	3,986	1,555	1,487
ρ (kJ/m^3)	11,033	10,681	11,033	10,681

5. CONCLUSIONS

Utilizing the compression heat to meet external space and water heating needs can significantly improve the efficiency of CAES technology. Our thermodynamic analysis reveals that waste heat recovery enhances the exergy efficiency of CAES from approximately 54% to 84%. Moreover, increasing the maximum cavern pressure lowers the exergy efficiency of CAES (due to higher compression losses) whereas it improves the D-CAES efficiency (due to increased waste heat recovery in addition to lower pipeline losses).

We recognize that the analysis presented here investigates solely the thermodynamic performance of D-CAES and neglects capital and operating costs. Nevertheless, the economic viability of D-CAES is expected to be determined by the trade-off between revenues from waste heat recovery and capital cost of the pipeline (strongly correlated with the pipeline length).

REFERENCES

[1] Succar, S. and R.H. Williams, Compressed air energy storage, theory, resources, and applications for wind power. 2008, Princeton Environmental Institute, Princeton University: Princeton, NJ.

[2] Knoke, S., Compressed air energy storage (CAES), in Handbook of energy storage for transmission or distribution applications, S. Eckroad, Editor. 2002, The Electric Power Research Institute (EPRI): Palo Alto, CA.
[3] Safaei, H., D.W. Keith, and R.J. Hugo, Compressed air energy storage (CAES) with compressors distributed at heat loads to enable waste heat utilization. Applied Energy, 2013. 103: p. 165-179.
[4] Hartmann, N., et al., Simulation and analysis of different adiabatic compressed air energy storage plant configurations. Applied Energy, 2012. 93: p. 541-548.
[5] Steta, F.D.S., Modeling of an advanced adiabatic compressed air energy storage (AA-CAES) unit and an optimal model-based operation strategy for its integration into power markets. 2010, Swiss Federal Institute of Technology (ETH) Zurich: Zurich.
[6] Wright, S., Reference design description and cost evaluation for compressed air energy storage systems. 2011, Electric Power Research Institute (EPRI): Palo Alto, CA.
[7] Compressed air energy storage power plants. 2007, FIZ Karlsruhe, German Federal Ministry of Economics and Technology: Bonn, Germany.
[8] ADELE – Adiabatic compressed-air energy storage (CAES) for electricity supply 2013, RWE Corp.
[9] Safaei, H. and D.W. Keith, Compressed air energy storage with waste heat export: An Alberta case study. Energy Conversion and Management, 2014. 78(0): p. 114-124.
[10] Osterle, J.F., The thermodynamics of compressed air exergy storage. Journal of Energy Resources Technology, 1991. 113(1): p. 7-11.
[11] Kim, Y.M. and D. Favrat, Energy and exergy analysis of a micro-compressed air energy storage and air cycle heating and cooling system. Energy, 2009. 35(1): p. 213-220.
[12] Grazzini, G. and A. Milazzo, Thermodynamic analysis of CAES/TES systems for renewable energy plants. Renewable Energy, 2008. 33(9): p. 1998-2006.
[13] Kim, Y.M., D.G. Shin, and D. Favrat, Operating characteristics of constant-pressure compressed air energy storage (CAES) system combined with pumped hydro storage based on energy and exergy analysis. Energy, 2011. 36(10): p. 6220-6233.
[14] Menon, S., Gas pipeline hydraulics. 2005, Boca Raton, FL: Taylor and Francis Group.
[15] Ummels, B.C., et al. Comparison of integration solutions for wind power in the Netherlands. 2009. Six Hills Way, Stevenage, SG1 2AY, United Kingdom: Institution of Engineering and Technology.
[16] Weber, O., Huntorf air storage gas turbine power plant. Brown Boveri Review, 1975. 62: p. 332-337.